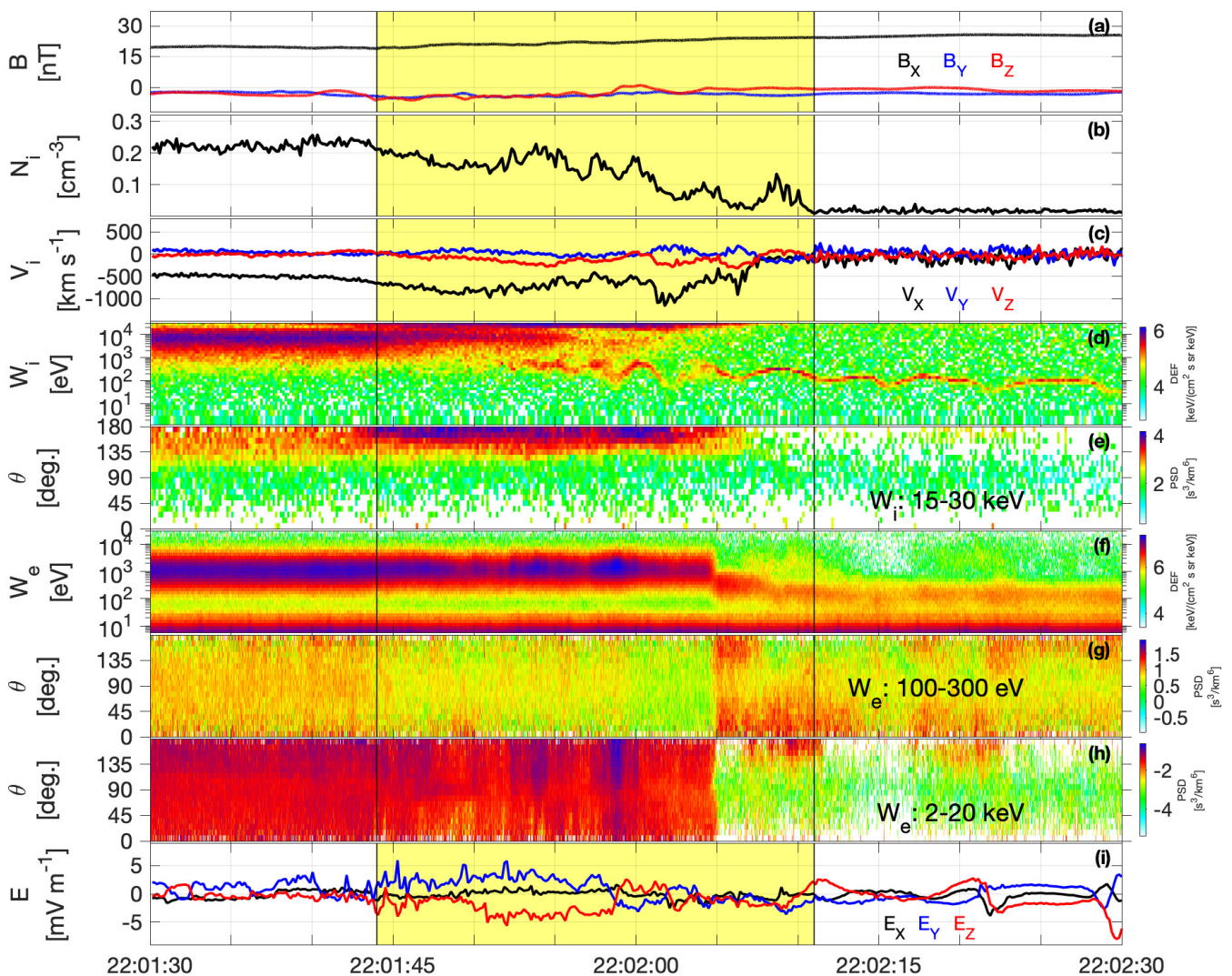


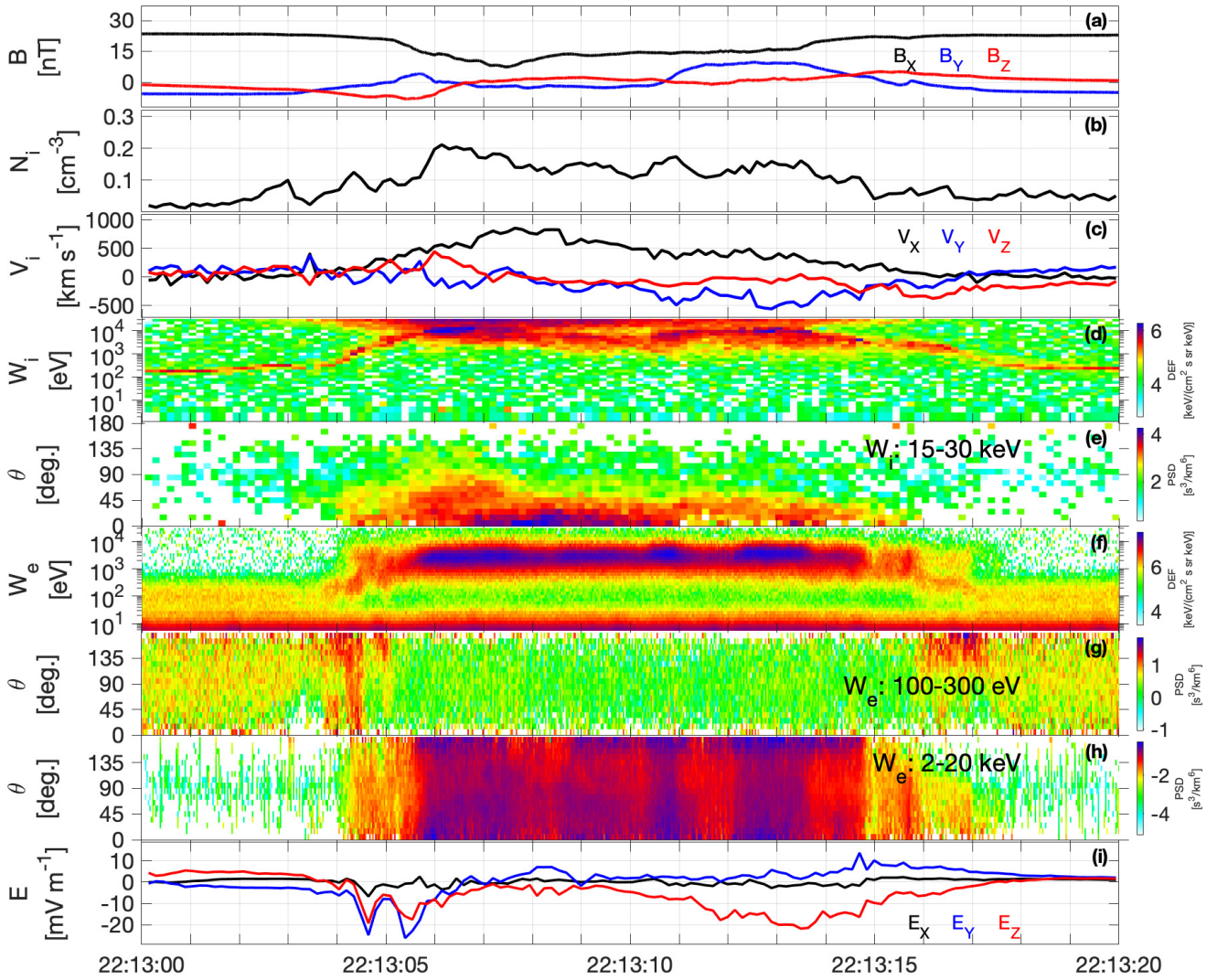
## Supplementary Material

### 1 SUPPLEMENTARY FIGURES

Figures S1 and S2 show the separatrix crossings of the tailward and earthward ion jets, respectively. MMS observe accelerated field-aligned ion and electron beams moving from the X line and low-energy electron beam moving towards the X line. Hall electric field, predominantly along  $-Z$  direction, points towards the neutral line. All those features indicate separatrix crossing of magnetic reconnection in the magnetotail. Cold ions of ionospheric origin are all observed from the lobe region to the separatrix boundary layer.



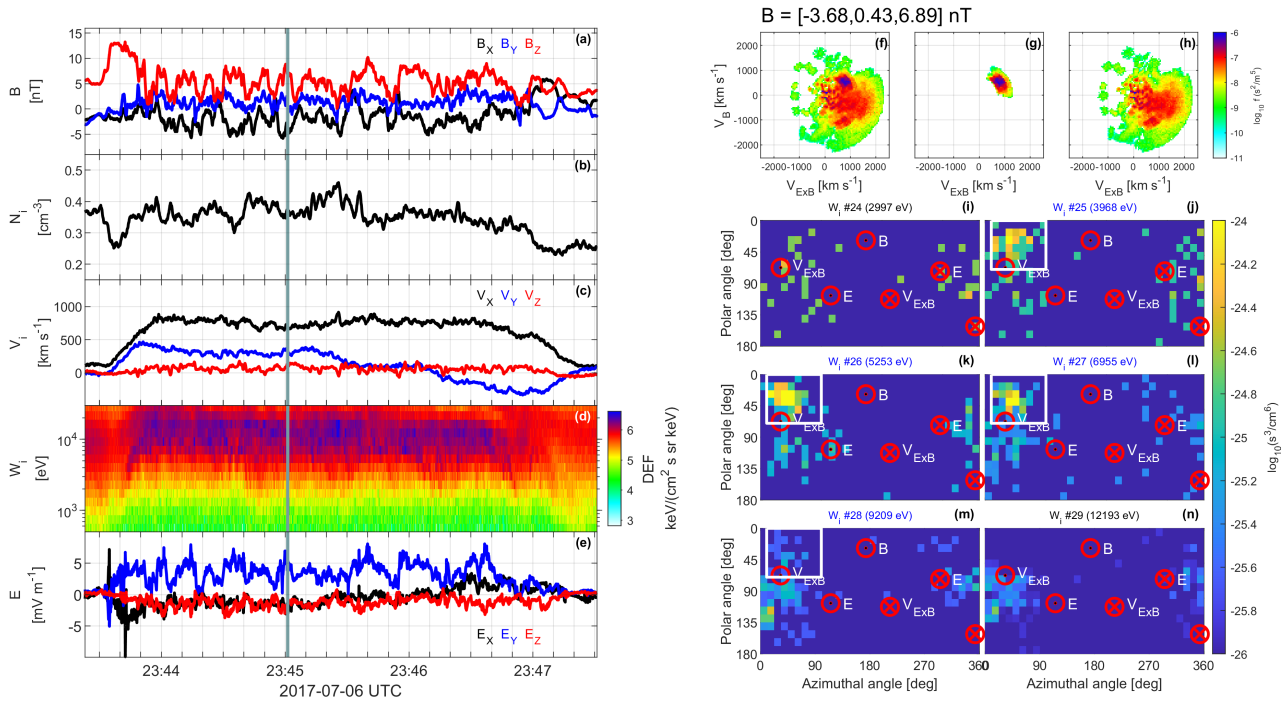
**Figure S1.** MMS1 observation between 22:01:30 UTC and 22:02:30 UTC showing a separatrix crossing. (a) Magnetic field  $\mathbf{B}$ . (b) Ion number density  $N_i$  from FPI. (c) Ion bulk velocity  $\mathbf{V}_i$  from FPI. (d) FPI ion omnidirectional differential energy flux. (e) 15-30 keV ion pitch-angle distribution in spacecraft frame. (f) FPI electron omnidirectional differential energy flux. (g) 100-300 eV and (h) 2-20 keV electron pitch-angle distributions. (i) Electric field  $\mathbf{E}$ . All the vectors are presented in Geocentric Solar Elliptic (GSE) coordinates. The yellow-shaded bar highlights the separatrix boundary.



**Figure S2.** MMS1 observation between 22:13:00 UTC and 22:13:20 UTC showing a back-and-forth separatrix crossing. The figure is in the same format with Figure S1.

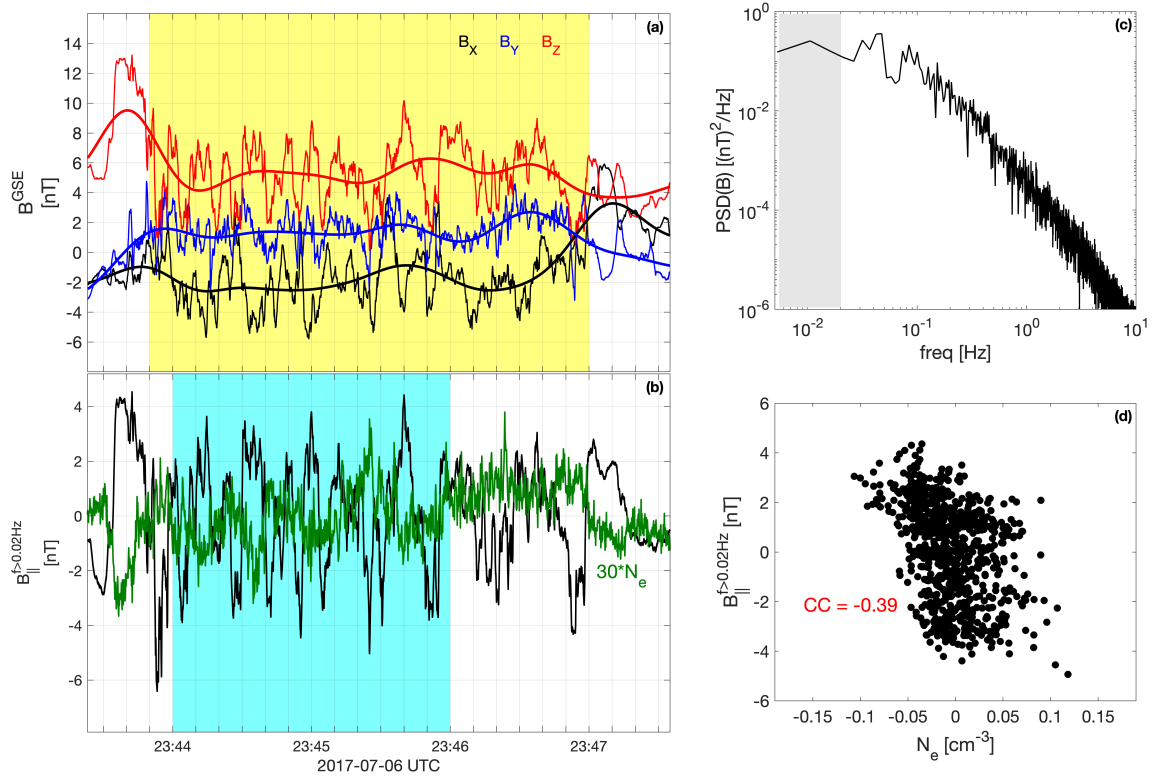
Figure S3 shows an example to separate the cold and hot populations from one FPI ion distribution function. Figures S3(a-e) present a summary figure of the MMS1 observation, and Fig. S3(f) displays a two-dimensional reduced ion VDF at the time indicated by the vertical line in Figs. S3(a-e). One can clearly see one hot and one cold populations close to the  $\mathbf{E} \times \mathbf{B}$  drift direction, and the cold population has large parallel velocity. We use a quadrilateral in Figs. S3(j-m) to separate the cold-ion beam from the hot plasma-sheet ion in the energy range from 3968 eV to 9209 eV, and the separated cold and hot VDFs are presented in Figs. S3(g-h), respectively.

Figure S4 shows the fluctuating magnetic field and plasma number density. The power-spectral density of the magnetic field has a power-law type shape and no clear strong power peak, suggesting turbulence-type nature of the magnetic field in this reconnection jet. The overall ion temperature anisotropy  $T_{i\perp}/T_{i\parallel} \sim 0.92$  is small. The cold-ion beam instability may not be satisfied locally. The observed fluctuations may be convected from the diffusion region. The low-band passed magnetic field with frequency below 0.02



**Figure S3.** An example showing how to separate different populations from one FPI distribution function. (a)  $\mathbf{B}$ . (b)  $N_i$ . (c)  $\mathbf{V}_i$ . (d) Ion omnidirectional differential energy flux. (e)  $\mathbf{E}$ . (f) Two-dimensional reduced ion VDF on  $V_{E \times B}$ - $V_B$  plane at the time indicated by the vertical line in (a-e). (g) Cold and (h) hot populations separated from (f). (i)-(n) Distribution function of (f) from 2997 eV to 12,193 eV, with the directions of  $\mathbf{B}$ ,  $\mathbf{E}$ , and  $\mathbf{E} \times \mathbf{B}$  drift. The white quadrilaterals in Panels (j-m) represent the angular limitation between 3968 eV and 9209 eV for separating the distribution function of the cold-ion beam.

Hz is presented by the thicker curves in Fig. S4a. We convert the high-frequency fluctuations into the field-aligned coordinate system based on the low-frequency  $\mathbf{B}$ , and the compressive (parallel) component of that is presented in Fig. S4b, which has weak correlation (-0.39) with the plasma number density. Here, we use electron number density  $N_e$  for correlation coefficient analysis because of its higher time resolution than  $N_i$ .



**Figure S4.** Fluctuating magnetic field and plasma number density. (a) Original and low-band ( $f < 0.02$  Hz) passed magnetic field. (b) Compressive component of high-band ( $f > 0.02$  Hz) passed magnetic field (black curve) and fluctuating electron number density (green curve, multiplied by 30). (c) Power-spectral density of magnetic field in the yellow-shaded interval in (a). The gray shadow denote the region with frequency  $f < 0.02$  Hz. (d) Scatter plot of  $N_e$  and compressive component of the fluctuating magnetic field. Their correlation coefficient is  $-0.39$ .